Seasonal iron depletion in temperate shelf seas

Antony J. Birchill[1] [ID], Angela Milne[1] [ID], E. Malcolm S. Woodward[2] [ID], Carolyn Harris[2], Amber Annett[3] [ID], Dagmara Rusiecka[4,5], Eric P. Achterberg[4,5] [ID], Martha Gledhill[4,5] [ID], Simon J. Ussher[1] [ID], Paul J. Worsfold[1] [ID], Walter Geibert[6] [ID], and Maeve C. Lohan[5] [ID]

[1]School of Geography, Earth and Environmental Sciences, University of Plymouth, Plymouth, UK, [2]Plymouth Marine Laboratory, Plymouth, UK, [3]School of Geoscience, University of Edinburgh, Edinburgh, UK, [4]GEOMAR Helmholtz Centre for Ocean Research, Kiel, Germany, [5]Ocean and Earth Science, National Oceanography Centre, University of Southampton, Southampton, UK, [6]Alfred Wegener Institute, Bremerhaven, Germany

Abstract Our study followed the seasonal cycling of soluble (SFe), colloidal (CFe), dissolved (DFe), total dissolvable (TDFe), labile particulate (LPFe), and total particulate (TPFe) iron in the Celtic Sea (NE Atlantic Ocean). Preferential uptake of SFe occurred during the spring bloom, preceding the removal of CFe. Uptake and export of Fe during the spring bloom, coupled with a reduction in vertical exchange, led to Fe deplete surface waters (<0.2 nM DFe; 0.11 nM LPFe, 0.45 nM TDFe, and 1.84 nM TPFe) during summer stratification. Below the seasonal thermocline, DFe concentrations increased from spring to autumn, mirroring NO_3^- and consistent with supply from remineralized sinking organic material, and cycled independently of particulate Fe over seasonal timescales. These results demonstrate that summer Fe availability is comparable to the seasonally Fe limited Ross Sea shelf and therefore is likely low enough to affect phytoplankton growth and species composition.

1. Introduction

Shelf seas cover <10% of the global ocean surface area yet contribute 10–20% of global oceanic primary production [*Muller-Karger et al.*, 2005]. Iron is an essential element for phytoplankton growth and hence plays a pivotal role in the functioning of marine ecosystems and the ocean carbon cycle [*Boyd and Ellwood*, 2010; *Twining and Baines*, 2013]. Shelf seas are assumed to be Fe replete due to riverine and groundwater inputs, sediment resuspension, and diagenetic supplies [e.g., *Chase et al.*, 2005; *Elrod et al.*, 2004; *Homoky et al.*, 2012; *Lohan and Bruland*, 2008; *Ussher et al.*, 2007]. However, seasonal Fe limitation has been demonstrated over narrow shelf regions of the Californian upwelling system [*Hutchins and Bruland*, 1998; *King and Barbeau*, 2007], in the Ross Sea [*Sedwick et al.*, 2011] and over the Bering Sea shelf break [*Aguilar-Islas et al.*, 2007]. Furthermore, the ability of an Atlantic coastal *Synechococcus* strain to alter its physiology in response to variable Fe availability [*Mackey et al.*, 2015], and expression of genes encoding flavodoxin in coastal diatoms [*Chappell et al.*, 2015], emphasizes the importance of understanding Fe availability to phytoplankton in dynamic shelf regions.

Evidence of Fe stress at elevated DFe concentrations (0.40–1.73 nM) [*Blain et al.*, 2004; *Chappell et al.*, 2015] highlights the need to consider not just DFe concentration but also the physicochemical speciation of Fe, which influences bioavailability [*Hassler and Schoemann*, 2009; *Hutchins et al.*, 1999; *Lis et al.*, 2015]. In shelf systems, particulate Fe dominates the total Fe inventory [*Hong and Kester*, 1986], where up to 81% can be in a labile particulate fraction [*Hurst et al.*, 2010]. This LPFe is considered available to phytoplankton, accessed directly from the particulate phase or indirectly following dissolution [*Chase et al.*, 2005; *Hurst et al.*, 2010; *Rubin et al.*, 2011]. Dissolved Fe can be further quantified in terms of SFe (<0.02 μm) and CFe (0.02–0.2 μm), with the CFe fraction found to comprise 60–80% of the DFe pool in continental shelf waters [*Hurst et al.*, 2010]. Dissimilar bioavailability of SFe and CFe has been demonstrated in laboratory studies [*Chen et al.*, 2003; *Chen and Wang*, 2001].

As part of the UK Shelf Sea Biogeochemistry programm (http://www.uk-ssb.org/), we investigated the cycling and distribution of the physicochemical speciation of Fe in the central Celtic Sea. As a seasonally stratifying shelf sea, the degree of vertical mixing determines the availability of light and nutrients to phytoplankton [*Pingree et al.*, 1976]. To date, research into Celtic Sea nutrient cycling has predominantly focused on the availability of NO_3^- to phytoplankton [*Hickman et al.*, 2012; *Pingree et al.*, 1976; *Sharples et al.*, 2001, 2009; *Williams et al.*, 2013], which is exhausted in surface waters following the onset of stratification and the phytoplankton
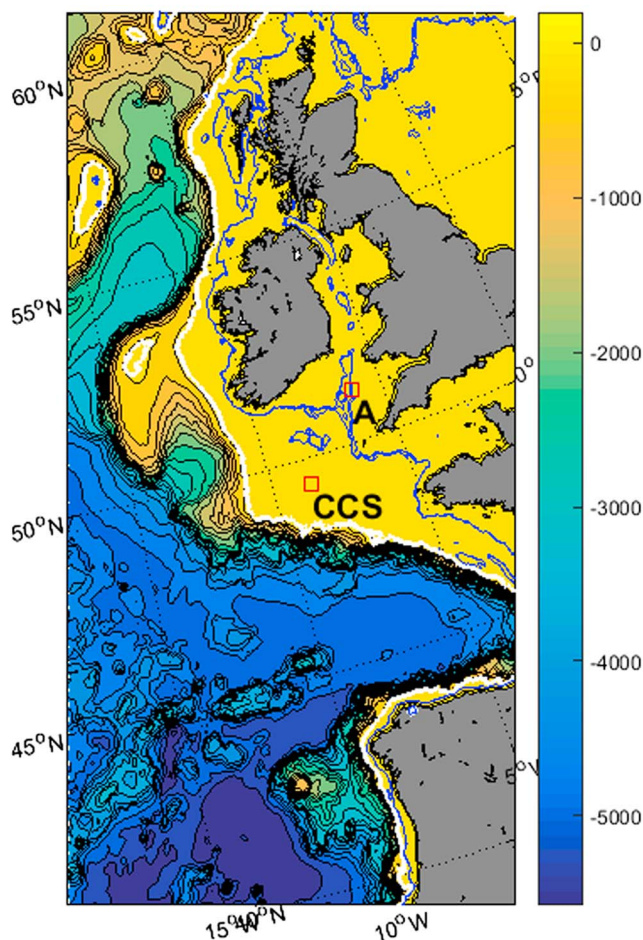
Figure 1. Map of Celtic Sea bathymetry (color bar, m), the white line is the 200 m isobath and blue line is the 100 m isobath, data provided by the *National Geophysical Data Center, N. N. U. S. D. C* [1995]. The central Celtic Sea (CCS) sampling site (49°24′N, 8°36′W), ~150 m depth, was the location of this study. Site A (51°12′N, 6°8′W), ~100 m depth, was the primary sampling site of the study conducted by *Klar et al.* [2017].

spring bloom in April. Here we show that all potentially available Fe sources were also drawn down to limiting concentrations in the surface mixed layer (SML), implying that this system is likely limited by both Fe and NO_3^-.

2. Methods

Sampling was conducted during three cruises (November 2014, April 2015, and July 2015) on board the *R.R.S. Discovery* at a central Celtic Sea station known as CCS (Figure 1). Full details of methods are provided in the supporting information S1, and a glossary of the Fe fractions are presented in Table 1. Briefly, all trace metal samples were collected following GEOTRACES protocols [*Cutter et al.*, 2010]. Dissolved Fe (0.2 μm filtered), SFe (0.02 μm filtered), and TDFe (unfiltered) were analyzed using flow injection with chemiluminesence detection [*Floor et al.*, 2015; *Obata et al.*, 1993], after spiking with hydrogen peroxide [*Lohan et al.*, 2006]. Colloidal Fe (0.02–0.2 μm) was determined by calculating the difference between the DFe and SFe concentrations. Particulate samples (≥0.45 μm) were collected on membrane filters and subjected to a sequential leach-digest procedure [*Milne et al.*, 2017]. The LPFe fraction was determined following protocols adapted from *Berger et al.* [2008] with 25% acetic acid as the leach reagent. For determination of total TPFe, a sequential acid digestion modified from *Ohnemus et al.* [2014] was used. All particulate digest samples were analyzed using inductively coupled plasma-mass spectrometry.

Nitrate plus nitrite (hereafter NO_3^-) concentrations were measured at sea using segmented flow techniques with spectrophotometric detection [*Brewer and Riley*, 1965; *Woodward and Rees*, 2001] and International

Table 1. A Glossary of the Operationally Defined Iron Fractions Determined During This Study[a]

Fraction	Abbreviation	Filtration	Iron Accessed
Dissolved Iron	DFe	<0.2 μm	Includes all iron passing through 0.2 μm filter that is dissolved after a minimum of 2 months at pH 1.6. This includes both soluble and colloidal phases (see below).
Soluble Iron	SFe	<0.02 μm	Includes all iron passing through 0.02 μm filter that is dissolved after a minimum of 2 months at pH 1.6. This includes free inorganic species and iron bound to low molecular weight organic complexes.
Colloidal Iron	CFe	dFe-sFe	Includes Fe in the size fraction 0.02–0.2 μm. Includes iron containing nanoparticles and iron bound to organic material in the colloidal phase, e.g., humic substances and polysaccharides.
Total Dissolvable Iron	TDFe	Unfiltered	Includes all iron dissolved from an unfiltered sample after a minimum of 6 months at pH 1.6. In this study concentrations were in excess of the sum of DFe and leachable particulate iron (see below), indicating that this treatment accessed refractory phases of particulate iron.
Leachable Particulate Iron	LPFe	>0.45 μm	Includes readily reducible iron oxyhydroxides and intracellular iron retained on a 0.45 μm filter.
Total Particulate Iron	TPFe	>0.45 μm	Includes all iron phases (refractory + leachable particulate iron) retained on a 0.45 μm filter.

	DFe (nM)	SFe (nM)	CFe (nM)	TDFe (nM)	LPFe (nM)	TPFe (nM)	NO_3^- (μM)
3–26 April 2015	0.23 ± 0.002 to 0.76 ± 0.009	0.11 ± 0.010 to 0.33 ± 0.000	0.13 ± 0.010 to 0.43 ± 0.010	6.84 ± 0.085[b] to 46.81 ± 1.267	3.47 ± 0.07[b] to 5.69 ± 0.04	44.82 ± 0.22[b] to 87.37 ± 0.90	1.15 to 6.03
14–31 July 2015	0.16 ± 0.071 (n = 15)	0.13 ± 0.069 (n = 3)	0.07 ± 0.092 (n = 3)	0.45 ± 0.179 (n = 14)	0.11 ± 0.003 (n = 1)	1.84 ± 0.010 (n = 1)	< 0.02 μM
11–29 November 2014	0.29 ± 0.068 (n = 9)	0.14 ± 0.082 (n = 3)	0.17 ± 0.036 (n = 3)	3.73 ± 0.583 (n = 6)	0.34 ± 0.024 (n = 2)	4.26 ± 0.251 (n = 2)	2.33 ± 0.037 (n = 14)

[a]Full details are provided in the supporting information S1. Concentrations of each fraction observed in surface waters are also displayed. For April 2015 the range of concentrations observed at 20 m are presented. For July 2015 the state of water column stratification was consistent and so the surface mixed layer was defined following *Hickman et al.* [2012]. In November 2014 the strength of stratification was variable and the surface mixed layer was determined by visual inspection of the profile.

[b]TDFe samples collected 12–26 April, LPFe and TPFe samples collected from 3 to 16 April.

GO-SHIP sampling and handling protocols [*Hydes et al.*, 2010]. Salinity, temperature, and depth were measured using a CTD system (Seabird 911+), equipped with optical backscatter, dissolved oxygen (O_2), and chlorophyll *a* (chl *a*) sensors which were calibrated daily [*Carritt and Carpenter*, 1966; *Holm-Hansen et al.*, 1965] on board ship.

Large seawater volumes (60–100 L) for determining radium (Ra) isotopes were pooled from Niskin bottles, and Ra extracted by adsorption onto manganese-impregnated acrylic fiber [*Sun and Torgersen*, 1998]. Radium activities were analyzed by Radium Delayed Coincidence Counting [*Annett et al.*, 2013; *Garcia-Solsona et al.*, 2008; *Moore*, 2008; *Moore and Arnold*, 1996] and corrected for supported activity from parent isotopes.

3. Results and Discussion

The central Celtic Sea is characterized by weak residual currents [*Pingree and Le Cann*, 1989] with a water residence time of 1–2 years [*Bailly Du Bois et al.*, 2002]. Consequently, by sampling over autumn (November 2014), spring (April 2015), and summer (July 2015) we were able to capture the seasonality of these waters over a 1 year cycle.

3.1. Conditions Following Winter Mixing

At the onset of seasonal stratification (3 April, 2015), the vertical distributions of DFe (0.82 ± 0.041 nM, n = 6) and NO_3^- (6.68 ± 0.370 μM, n = 14) were relatively uniform, with only minor evidence of surface drawdown, and thus reflecting winter mixing conditions and concentrations before the spring bloom (Figures 2a and 2b). In contrast, sediment resuspension increased the concentrations of TPFe and LPFe in near bottom samples (185.1 and 13.0 nM) relative to samples collected at 20 m (87.4 and 5.7 nM). At this time, CFe comprised 59–81% of DFe (Figures 2e and 2f), similar to the contributions observed near the north west Atlantic continental margin [*Fitzsimmons et al.*, 2015a] and shelf regions of the Bering Sea [*Hurst et al.*, 2010], though less variable than in the Canary basin [*Ussher et al.*, 2010]. The CFe ratio was greater than the ~50:50 partitioning observed in deep oceanic waters [*Fitzsimmons et al.*, 2015a; *Ussher et al.*, 2010]. Therefore, this suggests either enhanced input of colloidal material from sediment resuspension and/or from breakup of organic material, which particle reactive metals such as Fe associate with.
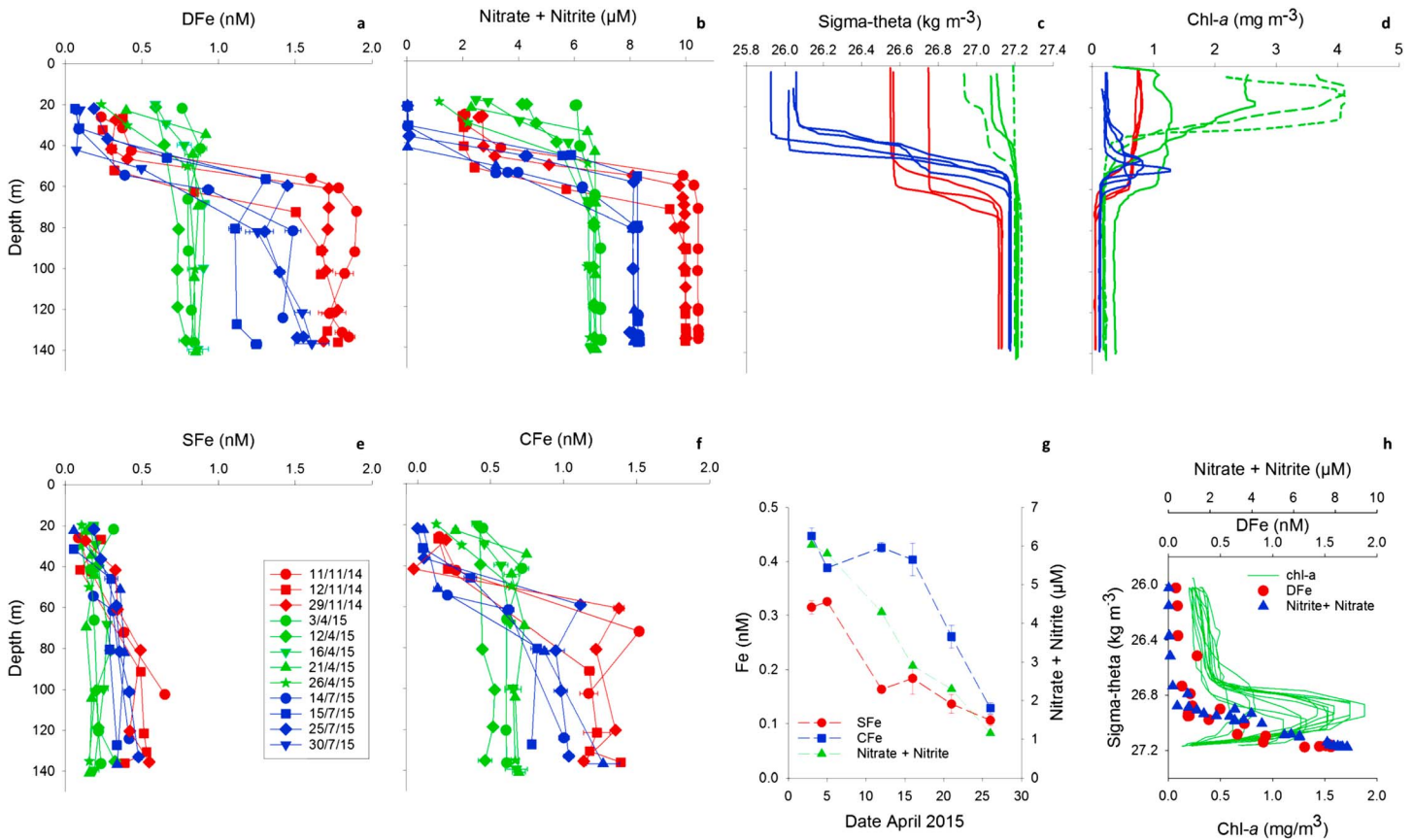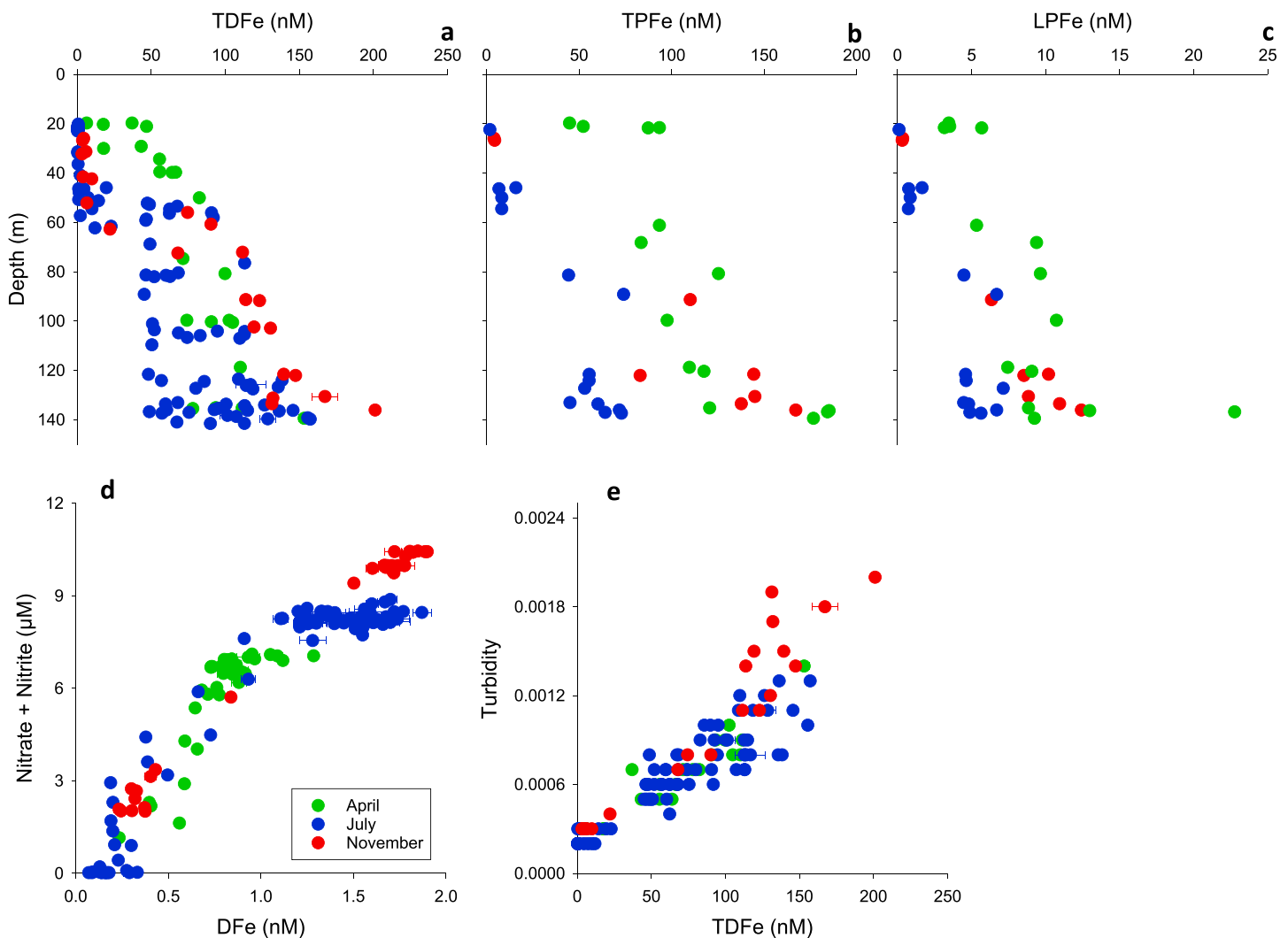
Figure 2. The seasonal time series of dFe at the Central Celtic Sea (CCS), November 2014 to July 2015. Top row relates (a) DFe to the oceanographic setting at the time of sampling, including the concentration of (b) NO_3^- (limit of detection 0.02 μM), the state of (c) stratification, indicated by sigma-theta, and (d) biomass, indicated by the chlorophyll a concentration. Sigma-theta plots are identified by the month of sampling only (red = November 14′, green = April 15′, and blue = July 15′), except the short dashed green line which represents the 3.4.15, from which point the surface density continuously decreased throughout April to the 26.4.15, represented by the large dashed green line. Chlorophyll a plots are identified by month of sampling (same color scheme as sigma-theta) except peak spring bloom chl a concentrations on 16.4.15 (short dashed line) and 21.4.15 (long dashed line). The bottom row includes the temporal evolution of (e) SFe and (f) CFe, which together make up DFe, shows the drawdown of SFe, CFe, and NO_3^- at 20 m depth during the spring bloom in (g) April 2015 and the concentration of DFe and NO_3^- in the pycnocline during (h) July 2015, in relation to the subsurface chlorophyll a maximum. The pycnocline region determined following *Hickman et al.* [2012]. Note that in July 2015, samples were collected for the determination of DFe during 14 casts′, for clarity only those with corresponding SFe concentrations are displayed. For the full range of DFe concentrations see Figure 3d.

3.2. Iron and Nitrate Uptake During the Spring Phytoplankton Bloom

During the phytoplankton spring bloom (3–26 April 2015), both DFe and NO_3^- were removed from the SML, where a depletion of 4.93 μM of NO_3^- at 20 m was observed (Figures 2b and 2g), consistent with published NO_3^- data [*Fasham et al.*, 1983]. Here we observed a 0.53 nM depletion of DFe as part of the first seasonal Fe data set for this region (Figures 2a and 2g). If all the DFe drawdown was a result of biological uptake this would equate to a phytoplankton Fe:N (nM:μM) ratio of 0.11; this calculation assumes no loss of DFe through scavenging and/or input via solubilization of LPFe. Nevertheless, the uptake ratio calculated here is within the range reported for cultured phytoplankton grown in Fe replete environments (0.05–0.9 nM Fe: μM N) [*Ho et al.*, 2003; *Sunda and Huntsman*, 1997], suggesting that phytoplankton species with a low to moderate Fe requirement would not have been affected by Fe stress during the spring bloom. Moreover, the concentration of the LPFe fraction, which is considered a bioavailable source of Fe [*Chase et al.*, 2005; *Hurst et al.*, 2010; *Milne et al.*, 2017], was 3.96 ± 1.16 nM (n = 4) at 20 m in April 2015 (Figure 3c) and decreased by ~2 nM from 3 to 16 April 2015.

Distinct temporal trends in the different size fractions of DFe were observed during the spring bloom. At the start of the bloom (5–12 April 2015), SFe decreased from 0.33 ± 0.000 to 0.16 ± 0.007 nM (Figure 2g). In contrast, the CFe concentration remained constant at 0.42 ± 0.026 nM (3–16 April 2015, n = 4; Figure 2g),

Figure 3. The seasonal time series of particulate iron in the central Celtic Sea, November 2014 to July 2015. Depth profiles of (a) TDFe, (b) PFe, and (c) LpFe. Bottom row displays close coupling between (d) DFe and NO_3^- ($r^2 = 0.94$) compared to the coupling between TDFe and particle load, as indicated by (e) turbidity (April $r^2 = 0.87$, July $r^2 = 0.86$, and November $r^2 = 0.92$).

suggesting that aggregation to the colloidal fraction was not a major removal pathway for sFe at this time, unless colloidal Fe was being removed at an equal rate to that of sFe aggregation. Therefore, these results suggest that phytoplankton preferentially utilized SFe during the initial stages of the bloom, consistent with laboratory culture studies [*Chen et al.*, 2003; *Chen and Wang*, 2001]. A decrease in CFe concentration from 0.40 ± 0.030 to 0.13 ± 0.010 nM (Figure 2g) occurred once the bloom had established (16–26 April 2015). Biological uptake of CFe by phytoplankton can occur, either directly [*Nodwell and Price*, 2001; *Rubin et al.*, 2011] or indirectly, following dissolution to the soluble phase by ligand/light interaction [*Borer et al.*, 2005; *Sulzberger et al.*, 1989] or grazing [*Schmidt et al.*, 2016]. Given the scarcity of SFe (<0.16 nM), and elevated primary production, at this time, it is probable that biological uptake contributed to the depletion of CFe in the SML. Preferential removal of SFe appears to contrast with observations in the open ocean, where preferential CFe uptake is hypothesized to be the cause of CFe minima in the deep chlorophyll maximum [*Fitzsimmons et al.*, 2015a]. Our spring bloom time series in a shelf environment allows us to suggest that SFe is the more bioavailable fraction as SFe uptake precedes the removal of CFe, and therefore, the observed CFe minima represents the net effect of SFe and CFe removal processes.

The observed time scale of CFe removal from the SML (~10 days) is consistent with the typically short residence times of colloidal thorium, which is in the order of hours to days in shelf waters [*Baskaran et al.*, 1992;

Moran and Buesseler, 1993]. This suggests that the decreasing CFe concentration reflected a change in the balance between sources and sinks of colloids over these time scales. In addition to biological uptake, both adsorption and coagulation of CFe lead to particle formation [*Honeyman and Santschi*, 1991] and potential export from the SML. Using profiles of excess radium activity (Ra$_{XS}$) (^{224}Ra$_{XS}$ half-live = 3.66 days, ^{223}Ra$_{XS}$ half-live = 11.4 days) as a tracer of vertical mixing (Figure S1), we show that increasing stratification progressively restricted vertical exchange with CFe-rich bottom waters, simultaneously reducing the supply of CFe to the SML.

3.3. Iron and Nitrate Availability During Summer Stratification

During summer stratification (July), the SML was depleted of both DFe (0.16 ± 0.071 nM, $n = 15$) and NO$_3^-$ (typically $<$0.02 μM) (Table 1 and Figures 2a–2c). As particulate Fe fractions were also quantified (Figure 3a–3c), we can consider all potentially bioavailable Fe sources. All particulate Fe fractions were lowest in the SML during summer (Table 1), including LPFe which was 0.11 ± 0.003 nM. The removal of LPFe, as well as DFe, indicated that all potentially bioavailable Fe sources were depleted in the SML of the central Celtic Sea and raises the question of whether primary production in the SML was seasonally colimited by Fe and NO$_3^-$ availability.

Analogous Fe cycling occurs in seasonally Fe-limited shelf regions of the southern Ross Sea. In these waters, winter convective overturning supplies both DFe and particulate Fe to surface waters. Subsequent biological uptake and export coupled with a reduction in vertical exchange leads to these waters becoming Fe limited in late spring/summer [*Marsay et al.*, 2014; *McGillicuddy et al.*, 2015; *Sedwick et al.*, 2011]. In contrast, the stratified central shelf waters of the Bering Sea maintain average summer SML LPFe concentrations of 6 nM, an important reservoir of bioavailable Fe for phytoplankton [*Hurst et al.*, 2010]. The central Celtic Sea represents an intermediate Fe cycle between these two environments. Unlike in the southern Ross Sea, complete NO$_3^-$ drawdown is observed during summer (Figure 2b), yet in this study the SML bioavailable Fe concentrations (DFe and LPFe; Figures 2a and 3c) were similar, and much lower than observed in the central Bering Sea. We hypothesize that the Celtic Sea ecosystem exists in a fine balance of Fe and NO$_3^-$ availability. Therefore, the structure of the summer ecosystem would be sensitive to changes in the availability of both nutrients. In the central Celtic Sea smaller species ($<$20 μm) dominate the summer phytoplankton community, with *Synechococcus* most abundant [*Sharples et al.*, 2007]. Small phytoplankton have a competitive advantage over larger phytoplankton in Fe deplete waters [*Lis et al.*, 2015]. Moreover, *Synechococcus* species has been shown to dominate in Fe-limited Southern Californian stratified coastal waters, where upon the addition of Fe the ecosystem shifted in favor of diatom growth [*Hopkinson and Barbeau*, 2008].

The DFe pool in the SML during July 2015 represents the Fe maintained through efficient recycling in [*Strzepek et al.*, 2005] in these nutrient poor waters. On average, the concentration of SFe (0.13 ± 0.069 nM $n = 3$) was in excess of the colloidal fraction (0.07 ± 0.092 nM, $n = 3$) (Figures 2e and 2f). Interestingly, these shelf concentrations were comparable to those seen in central oligotrophic gyres such as those observed at station ALOHA where SFe ranged from 0.05 to 0.1 nM in the upper 150 m, whereas CFe was depleted in the chlorophyll maximum [*Fitzsimmons et al.*, 2015b]. Although the concentration of SFe was low in both systems, it exceeded the solubility of the hydrolysis species [*Liu and Millero*, 2002]. Siderophores are low molecular weight complexes with high affinity and specificity for Fe(III) that are produced by marine bacterioplankton [*Gledhill et al.*, 2004], which may maintain the low, but persistent, SFe concentration in oligotrophic surface waters.

During summer months, the biomass maximum in the central Celtic Sea is observed below the SML, as a sub-surface chlorophyll maximum located in the pycnocline (Figures 2c and 2d). This is an important region of new production as phytoplankton are able to access the diapycnal flux of nutrients from the bottom mixed layer (BML) [*Hickman et al.*, 2012]. Within the pycnocline, zonation of phytoplankton species is driven by vertical gradients in light and NO$_3^-$ [*Hickman et al.*, 2009]. Here we observed a vertical gradient in DFe, NO$_3^-$ (Figure 2h) and photosynthetically available radiation of 16.4–0.11 W m^{-2} (during daytime casts). Photoacclimation at these light levels leads to increased cellular Fe quotas [*Strzepek and Price*, 2000; *Sunda and Huntsman*, 1997]. Where the flux of Fe across the pycnocline is insufficient to meet requirements, Fe and light colimitation influences phytoplankton species composition in the subsurface chlorophyll

maximum [*Hopkinson and Barbeau*, 2008; *Johnson et al.*, 2010]. The nutrient concentrations observed in these studies (dFe 0.11–1.10 nM and NO_3^- 0.3–6.5 μM) were similar to those observed at the July SCM in the central Celtic Sea (dFe 0.09–0.93 nM and NO_3^- 0.02–7.61 μM), indicating the potential for Fe/light colimitation. However, an estimate of the diffusive flux of DFe and NO_3^- through the thermocline indicated a DFe: NO_3^- (nM:μM) ratio of new production of 0.19 (supporting information S3). This is similar to the uptake ratio (0.11) observed during the spring bloom, suggesting that the growth of phytoplankton species with a low to moderate Fe requirement would be supported by this flux, though importantly this assumes complete biological utilization and no loss to scavenging. .

3.4. Iron and Nitrate Availability During the Autumn Phytoplankton Bloom

Water column stratification was also observed in autumn (November) (Figure 2c) and was reflected in the profiles of DFe, NO_3^-, and all particulate Fe fractions (Figures 2a, 2b, and 3a–3c). Radium activity profiles also showed complete depletion in the SML in November 2014 (Figure S1). The short half-lives of ^{223}Ra and ^{224}Ra indicate that rapid vertical exchange was still largely limited by the persistence of the seasonal pycnocline into November. Although still stratified, a net heat flux to the atmosphere meant stratification was progressively weakening relative to summer conditions [*Pingree et al.*, 1976] (Figure 2c). The relative increase in vertical exchange resulted in higher SML concentrations of bioavailable Fe and NO_3^- than observed during the summer stratified period (Table 1 and Figures 2a, 2b, and 3c). The increased supply of nutrients (including Fe) fueled an autumn bloom, observed here as elevated chl *a* concentrations of ~0.7 mg m^{-3} (Figure 2d).

3.5. Seasonal Cycling in the Bottom Mixed Layer

A seasonal buildup of DFe and NO_3^- in the BML (Figures 2a and 2b) occurred alongside an increase in dissolved inorganic carbon (DIC) (M. P. Humphreys, personal communication, 2017] and a decrease in dissolved oxygen (O_2) (Spring ~284 μM, Summer ~261 μM, and Autumn ~235 μM). The seasonal redistribution of NO_3^-, DIC, and O_2 was consistent with previous findings suggesting NO_3^- cycling was driven by uptake in the SML and subsequent remineralization in the BML [*Hickman et al.*, 2012; *Sharples et al.*, 2001]. When DFe concentrations from both the SML and BML (all seasons) are compared with corresponding NO_3^- concentrations a statistically significant relationship is noted ($r^2 = 0.94$, $p < 0.001$, $n = 163$; Figure 3d), suggesting that similar processes drive the observed seasonality of DFe. Moreover, an estimated 95% of the organic carbon present in Celtic Sea surface sediments is remineralized in repeated resuspension cycles rather than preserved [*de Haas et al.*, 2002]. Our results suggest that a similar process is occurring for the Fe associated with the organic matter. Additionally, no clear increase of DFe toward the seabed is observed in our profiles (Figure 2a) to suggest a significant diffusive sedimentary input of DFe. This is in contrast to a localized area in the north-eastern Celtic Sea where weaker current and wave activity permit the deposition of fine, organic-rich sediment [*de Haas et al.*, 2002; *McCave*, 1971], and a significant benthic source of DFe to the overlying water column was observed at the time of our study (Figure 1) [*Klar et al.*, 2017].

The majority (>99%) of DFe present in seawater is associated with organic complexes [*Gledhill and Buck*, 2012] which enhance the solubility of DFe in seawater above that of inorganic species [*Liu and Millero*, 2002]. Moreover, the concentration of organic-Fe chelators has been shown to control the solubility of Fe in particle-rich coastal and shelf waters [*Buck and Bruland*, 2007; *Buck et al.*, 2007]; in the BML the LPFe fraction (Figure 3c) was always in excess of DFe (Figure 2a). Partial remineralization of organic matter releases both DFe and organic Fe-binding complexes [*Boyd et al.*, 2010], which provides a potential mechanism for the seasonal increase in DFe concentrations. Temperature and pH also affect the solubility of Fe in seawater [*Liu and Millero*, 2002] and the binding strength of organic Fe-binding complexes [*Avendaño et al.*, 2016; *Gledhill et al.*, 2015] and could account for the seasonal buildup of dFe in the BML. The seasonal changes of temperature and pH in the BML were ~2°C and ~0.1 pH (M. P. Humphreys, personal communication, 2017) in the BML are thus considered insufficient to account for the seasonal buildup of DFe.

In contrast to DFe, the concentration of TDFe in the BML correlated with turbidity (Figure 3e), indicating that short-term resuspension events were the primary cause of high particulate Fe concentrations. Sediment resuspension events are driven by processes occurring on shorter time scales than seasonal changes (e.g., semidiurnal tides, internal tides, and storm events) and result in high particle loads in the BML of shelf systems relative to open ocean waters. Furthermore, the observed TPFe:TPAl molar ratio was seasonally invariant and ranged from 0.22 to 0.28, similar to the upper crustal ratio (0.19–0.23) [*McLennan*, 2001; *Rudnick*

and Gao, 2003; *Wedepohl*, 1995], and consistent with the majority of TPFe being supplied from a lithogenic source. Our results indicate that a large proportion of particulate Fe (~80%) is refractory (Figure 3b and 3c) and cycles independently of DFe. This is consistent with the majority of the Celtic Sea surface sediments being relict deposits from the Pleistocene and early Holocene, consisting of reworked, fine, and coarse sands [*de Haas et al*., 2002].

4. Conclusions

Our results show a seasonal, nutrient-type cycling of dFe in a temperate shelf sea. During summer, stratification isolates surface waters from Fe-rich bottom waters and provides a mechanism whereby temperate and high-latitude shelf sea ecosystems can become sensitive to Fe availability. The strength of seasonal stratification in North West European shelf seas is predicted to increase by ~20% by the end of the 21st century as a result of climate change [*Holt et al*., 2010]. Under these conditions the magnitude of the diapycnal nutrient flux, including dFe, will decrease, exacerbating the summer oligotrophic conditions. When assessing the effect this will have upon shelf sea primary production we assert that it is necessary to consider the role of Fe as potentially colimiting nutrient.

References

Aguilar-Islas, A. M., M. P. Hurst, K. N. Buck, B. Sohst, G. J. Smith, M. C. Lohan, and K. W. Bruland (2007), Micro-and macronutrients in the southeastern Bering Sea: Insight into iron-replete and iron-depleted regimes, *Prog. Oceanogr.*, *73*(2), 99–126, doi:10.1016/j.pocean.2006.12.002.

Annett, A. L., S. F. Henley, P. van Beek, M. Souhaut, R. Ganeshram, H. J. Venables, M. P. Meredith, and W. Geibert (2013), Use of radium isotopes to estimate mixing rates and trace sediment inputs to surface waters in northern Marguerite Bay, Antarctic Peninsula, *Antarct. Sci.*, *25*(03), 445–456, doi:10.1017/S0954102012000892.

Avendaño, L., M. Gledhill, E. P. Achterberg, V. M. C. Rérolle, and C. Schlosser (2016), Influence of ocean acidification on the organic complexation of iron and copper in northwest European shelf seas; a combined observational and model study, *Front. Mar. Sci.*, *3*, doi:10.3389/fmars.2016.00058.

Bailly Du Bois, P., P. Germain, M. Rozet, and L. Solier (2002), Water masses circulation and residence time in the Celtic Sea and English Channel approaches, characterisation based on radionuclides labelling from industrial releases, in *International Conference on Radioactivity in Environment*, edited by P. Borretzen, T. Jolle, and P. Strand, pp. 395–399, Monaco.

Baskaran, M., P. H. Santschi, G. Benoit, and B. Honeyman (1992), Scavenging of thorium isotopes by colloids in seawater of the Gulf of Mexico, *Geochim. Cosmochim. Acta*, *56*(9), 3375–3388, doi:10.1016/0016-7037(92)90385-V.

Berger, C. J., S. M. Lippiatt, M. G. Lawrence, and K. W. Bruland (2008), Application of a chemical leach technique for estimating labile particulate aluminum, iron, and manganese in the Columbia River plume and coastal waters off Oregon and Washington, *J. Geophys. Res.*, *113*, C00B01, doi:10.1029/2007JC004703.

Blain, S., C. Guieu, H. Claustre, K. Leblanc, T. Moutin, B. Quéguiner, J. Ras, and G. Sarthou (2004), Availability of iron and major nutrients for phytoplankton in the northeast Atlantic Ocean, *Limnol. Oceanogr.*, *49*(6), 2095–2104, doi:10.4319/lo.2004.49.6.2095.

Borer, P. M., B. Sulzberger, P. Reichard, and S. M. Kraemer (2005), Effect of siderophores on the light-induced dissolution of colloidal iron(III) (hydr)oxides, *Mar. Chem.*, *93*(2–4), 179–193, doi:10.1016/j.marchem.2004.08.006.

Boyd, P., E. Ibisanmi, S. Sander, K. Hunter, and G. Jackson (2010), Remineralization of upper ocean particles: Implications for iron biogeochemistry, *Limnol. Oceanogr.*, *55*(3), 1271, doi:10.4319/lo.2010.55.3.1271.

Boyd, P. W., and M. J. Ellwood (2010), The biogeochemical cycle of iron in the ocean, *Nat. Geosci.*, *3*(10), 675–682, doi:10.1038/ngeo964.

Brewer, P., and J. Riley (1965), The automatic determination of nitrate in sea water, paper presented at Deep Sea research and oceanographic abstracts, Elsevier.

Buck, K. N., and K. W. Bruland (2007), The physicochemical speciation of dissolved iron in the Bering Sea, Alaska, *Limnol. Oceanogr.*, *52*(5), 1800, doi:10.4319/lo.2007.52.5.1800.

Buck, K. N., M. C. Lohan, C. J. Berger, and K. W. Bruland (2007), Dissolved iron speciation in two distinct river plumes and an estuary: Implications for riverine iron supply, *Limnol. Oceanogr.*, *52*(2), 843–855, doi:10.4319/lo.2007.52.2.0843.

Carritt, D. E., and J. H. Carpenter (1966), Comparison and evaluation of currently employed modifications of the Winkler method for determining dissolved oxygen in seawater; a NASCO report, *J. Mar. Res.*, *24*, 286–318.

Chappell, P. D., L. P. Whitney, J. R. Wallace, A. I. Darer, S. Jean-Charles, and B. D. Jenkins (2015), Genetic indicators of iron limitation in wild populations of Thalassiosira Oceanica from the northeast Pacific Ocean, *ISME J.*, *9*(3), 592–602, doi:10.1038/ismej.2014.171.

Chase, Z., B. Hales, T. Cowles, R. Schwartz, and A. van Geen (2005), Distribution and variability of iron input to Oregon coastal waters during the upwelling season, *J. Geophys. Res.*, *110*, C10S12, doi:10.1029/2004JC002590.

Chen, M., and W.-X. Wang (2001), Bioavailability of natural colloid-bound iron to marine plankton: Influences of colloidal size and aging, *Limnol. Oceanogr.*, *46*(8), 1956–1967.

Chen, M., R. C. H. Dei, W.-X. Wang, and L. Guo (2003), Marine diatom uptake of iron bound with natural colloids of different origins, *Mar. Chem.*, *81*(3–4), 177–189, doi:10.1016/S0304-4203(03)00032-X.

Cutter, G., P. Andersson, L. Codispoti, P. Croot, R. Francois, M. Lohan, H. Obata, and M. Rutgers vd Loeff (2010), Sampling and sample-handling protocols for GEOTRACES Cruises, 10013/epic.42722.

de Haas, H., T. C. E. van Weering, and H. de Stiger (2002), Organic carbon in shelf seas: Sinks or sources, processes and products, *Cont. Shelf Res.*, *22*(5), 691–717, doi:10.1016/S0278-4343(01)00093-0.

Elrod, V. A., W. M. Berelson, K. H. Coale, and K. S. Johnson (2004), The flux of iron from continental shelf sediments: A missing source for global budgets, *Geophys. Res. Lett.*, *31*, L12307, doi:10.1029/2004GL020216.

Fasham, M. J. R., P. M. Holligan, and P. R. Pugh (1983), The spatial and temporal development of the spring phytoplankton bloom in the Celtic Sea, April 1979, *Prog. Oceanogr.*, *12*(1), 87–145, doi:10.1016/0079-6611(83)90007-1.

Fitzsimmons, J. N., G. G. Carrasco, J. Wu, S. Roshan, M. Hatta, C. I. Measures, T. M. Conway, S. G. John, and E. A. Boyle (2015a), Partitioning of dissolved iron and iron isotopes into soluble and colloidal phases along the GA03 GEOTRACES North Atlantic Transect, *Deep Sea Res., Part II*, *116*, 130–151, doi:10.1016/j.dsr2.2014.11.014.

Fitzsimmons, J. N., C. T. Hayes, S. N. Al-Subiai, R. Zhang, P. L. Morton, R. E. Weisend, F. Ascani, and E. A. Boyle (2015b), Daily to decadal variability of size-fractionated iron and iron-binding ligands at the Hawaii Ocean Time-series Station ALOHA, *Geochim. Cosmochim. Acta*, *171*, 303–324.

Floor, G. H., R. Clough, M. C. Lohan, S. J. Ussher, P. J. Worsfold, and C. R. Quétel (2015), Combined uncertainty estimation for the determination of the dissolved iron amount content in seawater using flow injection with chemiluminescence detection, *Limnol. Oceanogr. Methods*, *13*(12), 673–686, doi:10.1002/lom3.10057.

Garcia-Solsona, E., J. Garcia-Orellana, P. Masqué, and H. Dulaiova (2008), Uncertainties associated with ^{223} Ra and ^{224} Ra measurements in water via a Delayed Coincidence Counter (RaDeCC), *Mar. Chem.*, *109*(3), 198–219.

Gledhill, M., and K. N. Buck (2012), The organic complexation of iron in the marine environment: A review, *Front. Microbiol.*, *3*, doi:10.3389/fmicb.2012.00069.

Gledhill, M., P. McCormack, S. Ussher, E. P. Achterberg, R. F. C. Mantoura, and P. J. Worsfold (2004), Production of siderophore type chelates by mixed bacterioplankton populations in nutrient enriched seawater incubations, *Mar. Chem.*, *88*(1), 75–83.

Gledhill, M., E. P. Achterberg, K. Li, K. N. Mohamed, and M. J. Rijkenberg (2015), Influence of ocean acidification on the complexation of iron and copper by organic ligands in estuarine waters, *Mar. Chem.*, *177*, 421–433.

Hassler, C., and V. Schoemann (2009), Bioavailability of organically bound Fe to model phytoplankton of the Southern Ocean, *Biogeosciences*, *6*(10), 2281–2296.

Hickman, A. E., P. M. Holligan, C. M. Moore, J. Sharples, V. Krivtsov, and M. R. Palmer (2009), Distribution and chromatic adaptation of phytoplankton within a shelf sea thermocline, *Limnol. Oceanogr.*, *54*(2), 525–536, doi:10.4319/lo.2009.54.2.0525.

Hickman, A. E., C. M. Moore, J. Sharples, M. I Lucas, G. H. Tilstone, V. Krivtsov, and P. M. Holligan (2012), Primary production and nitrate uptake within the seasonal thermocline of a stratified shelf sea, *Mar. Ecol. Prog. Ser.*, *463*, 39–57.

Ho, T. Y., A. Quigg, Z. V. Finkel, A. J. Milligan, K. Wyman, P. G. Falkowski, and F. M. Morel (2003), The elemental composition of some marine phytoplankton, *J. Phycol.*, *39*(6), 1145–1159.

Holm-Hansen, O., C. J. Lorenzen, R. W. Holmes, and J. D. Strickland (1965), Fluorometric determination of chlorophyll, *J. Conseil.*, *30*(1), 3–15.

Holt, J., S. Wakelin, J. Lowe, and J. Tinker (2010), The potential impacts of climate change on the hydrography of the northwest European continental shelf, *Prog. Oceanogr.*, *86*(3–4), 361–379, doi:10.1016/j.pocean.2010.05.003.

Homoky, W. B., S. Severmann, J. McManus, W. M. Berelson, T. E. Riedel, P. J. Statham, and R. A. Mills (2012), Dissolved oxygen and suspended particles regulate the benthic flux of iron from continental margins, *Mar. Chem.*, *134*, 59–70.

Honeyman, B. D., and P. H. Santschi (1991), Coupling adsorption and particle aggregation: Laboratory studies of "colloidal pumping" using iron-59-labeled hematite, *Environ. Sci. Technol.*, *25*(10), 1739–1747.

Hong, H., and D. R. Kester (1986), Redox state of iron in the offshore waters of Peru, *Limnol. Oceanogr.*, *31*(3), 512–524.

Hopkinson, B. M., and K. A. Barbeau (2008), Interactive influences of iron and light limitation on phytoplankton at subsurface chlorophyll maxima in the eastern North Pacific, *Limnol. Oceanogr.*, *53*(4), 1303–1318, doi:10.4319/lo.2008.53.4.1303.

Hurst, M. P., A. M. Aguilar-Islas, and K. W. Bruland (2010), Iron in the southeastern Bering Sea: Elevated leachable particulate Fe in shelf bottom waters as an important source for surface waters, *Cont. Shelf Res.*, *30*(5), 467–480.

Hutchins, D. A., and K. W. Bruland (1998), Iron-limited diatom growth and Si:N uptake ratios in a coastal upwelling regime, *Nature*, *393*(6685), 561–564.

Hutchins, D. A., A. E. Witter, A. Butler, and G. W. Luther (1999), Competition among marine phytoplankton for different chelated iron species, *Nature*, *400*(6747), 858–861.

Hydes, D., M. Aoyama, A. Aminot, K. Bakker, S. Becker, S. Coverly, A. Daniel, A. Dickson, O. Grosso, and R. Kerouel (2010), Determination of dissolved nutrients (N, P, Si) in seawater with high precision and inter-comparability using gas-segmented continuous flow analysers, The GO-SHIP Repeat Hydrography Manual: A collection of expert reports and guidelines; IOCCP report No.14, ICPO publication series No. 134, version 1.

Johnson, Z. I., R. Shyam, A. E. Ritchie, C. Mioni, V. P. Lance, J. W. Murray, and E. R. Zinser (2010), The effect of iron-and light-limitation on phytoplankton communities of deep chlorophyll maxima of the western Pacific Ocean, *J. Mar. Res.*, *68*(2), 283–308.

King, A. L., and K. Barbeau (2007), Evidence for phytoplankton iron limitation in the southern California Current System, *Mar. Ecol. Prog. Ser.*, *342*, 91–103.

Klar, J., W. B. Homoky, P. J. Statham, A. J. Birchill, E. Harris, E. M. S. Woodward, B. Silburn, M. Cooper, R. H. James, and D. P. Connelly (2017), Stability of dissolved and soluble Fe (II) in shelf sediment pore waters and release to an oxic water column, *Biogeochemistry*, doi:10.1007/s10533-017-0309-x.

Lis, H., Y. Shaked, C. Kranzler, N. Keren, and F. M. M. Morel (2015), Iron bioavailability to phytoplankton: An empirical approach, *ISME J.*, *9*(4), 1003–1013, doi:10.1038/ismej.2014.199.

Liu, X., and F. J. Millero (2002), The solubility of iron in seawater, *Mar. Chem.*, *77*(1), 43–54.

Lohan, M. C., and K. W. Bruland (2008), Elevated Fe (II) and dissolved Fe in hypoxic shelf waters off Oregon and Washington: An enhanced source of iron to coastal upwelling regimes, *Environ. Sci. Technol.*, *42*(17), 6462–6468.

Lohan, M. C., A. M. Aguilar-Islas, and K. W. Bruland (2006), Direct determination of iron in acidified (pH 1.7) seawater samples by flow injection analysis with catalytic spectrophotometric detection: Application and intercomparison, *Limnol. Oceanogr. Methods*, *4*(6), 164–171, doi:10.4319/lom.2006.4.164.

Mackey, K. R., A. F. Post, M. R. McIlvin, G. A. Cutter, S. G. John, and M. A. Saito (2015), Divergent responses of Atlantic coastal and oceanic Synechococcus to iron limitation, *Proc. Natl. Acad. Sci.*, *112*(32), 9944–9949.

Marsay, C. M., P. N. Sedwick, M. S. Dinniman, P. M. Barrett, S. L. Mack, and D. J. McGillicuddy (2014), Estimating the benthic efflux of dissolved iron on the Ross Sea continental shelf, *Geophys. Res. Lett.*, *41*, 7576–7583, doi:10.1002/2014GL061684.

McCave, I. N. (1971), Wave effectiveness at the sea bed and its relationship to bed-forms and deposition of mud, *J. Sediment. Res.*, *41*(1), 89–96, doi:10.1306/74d721f3-2b21-11d7-8648000102c1865d.

McGillicuddy, D. J., P. N. Sedwick, M. Dinniman, K. R. Arrigo, T. S. Bibby, B. J. Greenan, E. E. Hofmann, J. M. Klinck, W. O. Smith, and S. Mack (2015), Iron supply and demand in an Antarctic shelf ecosystem, *Geophys. Res. Lett.*, *42*, 8088–8097, doi:10.1002/2015GL065727.

McLennan, S. M. (2001), Relationships between the trace element composition of sedimentary rocks and upper continental crust, *Geochem. Geophys. Geosyst.*, *2*(4), 1021, doi:10.1029/2000GC000109.

Milne, A., C. Schlosser, B. D. Wake, E. P. Achterberg, R. Chance, A. Baker, A. Forryan, and M. C. Lohan (2017), Particulate phases are key in controlling dissolved iron concentrations in the (sub)-tropical North Atlantic, *Geophys. Res. Lett.*, *44*, 2377–2387, doi:10.1002/2016GL072314.

Moore, W. S. (2008), Fifteen years experience in measuring ^{224}Ra and ^{223}Ra by delayed-coincidence counting, *Mar. Chem.*, *109*(3), 188–197.

Moore, W. S., and R. Arnold (1996), Measurement of ^{223}Ra and ^{224}Ra in coastal waters using a delayed coincidence counter, *J. Geophys. Res.*, *101*, 1321–1329, doi:10.1029/95JC03139.

Moran, B. S., and K. O. Buesseler (1993), Size-fractionated ^{234}Th in continental shelf waters off New England: Implications for the role of colloids in oceanic trace metal scavenging, *J. Mar. Res.*, *51*(4), 893–922.

Muller-Karger, F. E., R. Varela, R. Thunell, R. Luerssen, C. Hu, and J. J. Walsh (2005), The importance of continental margins in the global carbon cycle, *Geophys. Res. Lett.*, *32*, L01602, doi:10.1029/2004GL021346.

National Geophysical Data Center, N. N. U. S. D. C (1995), *TerrainBase, Global 5 Arc-minute Ocean Depth and Land Elevation from the US National Geophysical Data Center (NGDC)*, Res. Data Arch. at the Natl. Cent. for Atmos. Res., Comput. and Inf. Syst. Lab., Boulder, Colo.

Nodwell, L. M., and N. M. Price (2001), Direct use of inorganic colloidal iron by marine mixotrophic phytoplankton, *Limnol. Oceanogr.*, *46*(4), 765–777, doi:10.4319/lo.2001.46.4.0765.

Obata, H., H. Karatani, and E. Nakayama (1993), Automated determination of iron in seawater by chelating resin concentration and chemiluminescence detection, *Anal. Chem.*, *65*(11), 1524–1528, doi:10.1021/ac00059a007.

Ohnemus, D. C., M. E. Auro, R. M. Sherrell, M. Lagerstrom, P. L. Morton, B. S. Twining, S. Rauschenberg, and P. J. Lam (2014), Laboratory intercomparison of marine particulate digestions including piranha: A novel chemical method for dissolution of polyethersulfone filters, *Limnol. Oceanogr. Methods*, *12*, 530–547.

Pingree, R., P. Holligan, G. Mardell, and R. Head (1976), The influence of physical stability on spring, summer and autumn phytoplankton blooms in the Celtic Sea, *J. Mar. Biol. Assoc. U. K.*, *56*(04), 845–873.

Pingree, R. D., and B. Le Cann (1989), Celtic and Armorican slope and shelf residual currents, *Prog. Oceanogr.*, *23*(4), 303–338, doi:10.1016/0079-6611(89)90003-7.

Rubin, M., I. Berman-Frank, and Y. Shaked (2011), Dust-and mineral-iron utilization by the marine dinitrogen-fixer Trichodesmium, *Nat. Geosci.*, *4*(8), 529–534.

Rudnick, R. L., and S. Gao (2003), 3.01—Composition of the Continental Crust A2—Holland, Heinrich D, in *Treatise on Geochemistry*, edited by K. K. Turekian, pp. 1–64, Pergamon, Oxford, doi:10.1016/B0-08-043751-6/03016-4.

Schmidt, K., C. Schlosser, A. Atkinson, S. Fielding, H. J. Venables, C. M. Waluda, and E. P. Achterberg (2016), Zooplankton gut passage mobilizes lithogenic iron for ocean productivity, *Curr. Biol.*, *26*(19), 2667–2673.

Sedwick, P. N., C. M. Marsay, B. M. Sohst, A. M. Aguilar Islas, M. Lohan, M. C. Long, K. R. Arrigo, R. B. Dunbar, M. A. Saito, and W. O. Smith (2011), Early season depletion of dissolved iron in the Ross Sea polynya: Implications for iron dynamics on the Antarctic continental shelf, *J. Geophys. Res.*, *116*, C12019, doi:10.1029/2010JC006553.

Sharples, J., C. M. Moore, A. E. Hickman, P. M. Holligan, J. F. Tweddle, M. R. Palmer, and J. H. Simpson (2009), Internal tidal mixing as a control on continental margin ecosystems, *Geophys. Res. Lett.*, *36*, L23603, doi:10.1029/2009GL040683.

Sharples, J., M. C. Moore, T. P. Rippeth, P. M. Holligan, D. J. Hydes, N. R. Fisher, and J. H. Simpson (2001), Phytoplankton distribution and survival in the thermocline, *Limnol. Oceanogr.*, *46*(3), 486–496.

Sharples, J., J. F. Tweddle, J. Mattias Green, M. R. Palmer, Y.-N. Kim, A. E. Hickman, P. M. Holligan, C. Moore, T. P. Rippeth, and J. H. Simpson (2007), Spring-neap modulation of internal tide mixing and vertical nitrate fluxes at a shelf edge in summer, *Limnol. Oceanogr.*, *52*(5), 1735–1747.

Strzepek, R., M. Maldonado, J. Higgins, J. Hall, K. Safi, S. Wilhelm, and P. Boyd (2005), Spinning the "ferrous wheel": The importance of the microbial community in an iron budget during the FeCycle experiment, *Global Biogeochem. Cycles*, *19*, GB4S26, doi:10.1029/2005GB002490.

Strzepek, R., and N. Price (2000), Influence of irradiance and temperature on the iron content of the marine diatom Thalassiosira Weissflogii (Bacillariophyceae), *Mar. Ecol. Prog. Ser.*, *206*, 107–117.

Sulzberger, B., D. Suter, C. Siffert, S. Banwart, and W. Stumm (1989), Dissolution of fe(III)(hydr)oxides in natural waters; laboratory assessment on the kinetics controlled by surface coordination, *Mar. Chem.*, *28*(1), 127–144, doi:10.1016/0304-4203(89)90191-6.

Sun, Y., and T. Torgersen (1998), The effects of water content and Mn-fiber surface conditions on ^{224}Ra measurement by ^{220}Rn emanation, *Mar. Chem.*, *62*(3), 299–306.

Sunda, W. G., and S. A. Huntsman (1997), Interrelated influence of iron, light and cell size on marine phytoplankton growth, *Nature*, *390*(6658), 389–392.

Twining, B. S., and S. B. Baines (2013), The trace metal composition of marine phytoplankton, *Annu. Rev. Mar. Sci.*, *5*, 191–215.

Ussher, S. J., P. J. Worsfold, E. P. Achterberg, A. Laës, S. Blain, P. Laan, and H. J. De Baar (2007), Distribution and redox speciation of dissolved iron on the European continental margin, *Limnol. Oceanogr. Methods*, *52*(6), 2530–2539.

Ussher, S. J., E. P. Achterberg, G. Sarthou, P. Laan, H. J. W. de Baar, and P. J. Worsfold (2010), Distribution of size fractionated dissolved iron in the Canary Basin, *Mar. Environ. Res.*, *70*(1), 46–55, doi:10.1016/j.marenvres.2010.03.001.

Wedepohl, H. K. (1995), The composition of the continental crust, *Geochim. Cosmochim. Acta*, *59*(7), 1217–1232.

Williams, C., J. Sharples, C. Mahaffey, and T. Rippeth (2013), Wind driven nutrient pulses to the subsurface chlorophyll maximum in seasonally stratified shelf seas, *Geophys. Res. Lett.*, *40*, 5467–5472, doi:10.1002/2013GL058171.

Woodward, E., and A. Rees (2001), Nutrient distributions in an anticyclonic eddy in the northeast Atlantic Ocean, with reference to nanomolar ammonium concentrations, *Deep Sea Res., Part II*, *48*(4), 775–793.